A possible mechanism for magnetar soft X-ray/γ-ray emission*

Gao Zhi-Fu(高志福)[a)b)c)], Peng Qiu-He(彭秋和)[d)†],
Wang Na(王 娜)[a)b)], and Chou Chih-Kang(邹志刚)[e)]

[a)] *Xinjiang Astronomical Observatory, Chinese Academy of Sciences, Urumqi* 830011, *China*
[b)] *Key Laboratory of Radio Astronomy, Chinese Academy of Sciences, Nanjing* 210008, *China*
[c)] *Graduate University of the Chinese Academy of Sciences, Beijing* 100080, *China*
[d)] *Department of Astronomy, Nanjing University, Nanjing* 210093, *China*
[e)] *National Astronomical Observatories, Chinese Academy of Sciences, Beijing* 100012, *China*

(Received 24 September 2011; revised manuscript received 12 December 2011)

Once the energies of electrons near the Fermi surface obviously exceed the threshold energy of the inverse β decay, electron capture (EC) dominates inside the magnetar. Since the maximal binding energy of the $^3P_2$ neutron Cooper pair is only about 0.048 MeV, the outgoing high-energy neutrons ($E_k(n) > 60$ MeV) created by the EC can easily destroy the $^3P_2$ neutron Cooper pairs through the interaction of nuclear force. In the anisotropic neutron superfluid, each $^3P_2$ neutron Cooper pair has magnetic energy $2\mu_n B$ in the applied magnetic field B, where $\mu_n = 0.966 \times 10^{-23}$ erg·G^{-1} is the absolute value of the neutron abnormal magnetic moment. While being destroyed by the high-energy EC neutrons, the magnetic moments of the $^3P_2$ Cooper pairs are no longer arranged in the paramagnetic direction, and the magnetic energy is released. This released energy can be transformed into thermal energy. Only a small fraction of the generated thermal energy is transported from the interior to the surface by conduction, and then it is radiated in the form of thermal photons from the surface. After highly efficient modulation within the star's magnetosphere, the thermal surface emission is shaped into a spectrum of soft X-rays/γ-rays with the observed characteristics of magnetars. By introducing related parameters, we calculate the theoretical luminosities of magnetars. The calculation results agree well with the observed parameters of magnetars.

Keywords: Landau levels, Fermi surface, thermal radiation, heat conduction

PACS: 71.70.Di, 71.18.+y **DOI:** 10.1088/1674-1056/21/5/057109

1. Introduction

Observational evidences for neutron stars (NSs) with strong surface dipole magnetic fields ($B \sim 10^{14}-10^{15}$ G), known as magnetars,[1] have steadily grown over the last decade. Magnetars are historically divided into two populations, which are independently discovered through different manifestations of their high-energy emissions. One is the soft gamma repeaters (SGRs), which give sporadic bursts of hard X-rays/soft γ-rays as well as rare, very luminous ($\sim 10^{44}$ erg $\cdot$ s^{-1}, 1 erg $= 10^{-7}$ J) giant flares. The other is the anomalous X-ray pulsars (AXPs), so called due to their high X-ray luminosities (10^{32}–10^{36} erg·s^{-1}) and unusually fast spin-down rates with no evidence of variation due to the binary motion, which are distinct from both the accreting X-ray binaries and the isolated radio pulsars.

With respect to the origin of the magnetic fields of the magnetars, the most popular assumption is that the rapid differential rotation and convection results in an efficient α–Ω dynamo.[1–3] However, there is no mechanism to explain such a high efficiency of energy transformation in the α–Ω dynamo model. Moreover, when investigating a solar flare by using this model, apart from the difficulty in explaining the high energy transformation efficiency, there are still many other problems that need to be settled.[4,5] Superhigh magnetic fields may originate from the paramagnetic fields produced by the aligned magnetic moments of

*Project supported by the National Natural Science Foundation of China (Grant No. 10773005), the National Basic Research Program of China (Grant No. 2009CB824800), the Knowledge Innovation Program of the Chinese Academy of Sciences (Grant No. KJCX$_2$-YW-T09), and the Key Directional Project of the Chinese Academy of Sciences and the National Natural Science Foundation of China (Grant Nos. 10173020, 10673021, 10778631 and 10903019).

†Corresponding author. E-mail: qhpeng@nju.edu.cn

© 2012 Chinese Physical Society and IOP Publishing Ltd

the $^3P_2$ neutron Cooper pairs, and the maximum of the paramagnetic fields is estimated to be about (3.0–4.0)$\times 10^{15}$ G.[6,7]

Magnetars have rather soft X-ray spectra ($kT <$ 10 keV) that are well fitted by a black-body model with a temperature of $kT \sim 0.5$ keV and a power-law tail with photon index $\Gamma \sim$3–4.[8] In a few magnetars, good fits are obtained equivalently by using two black bodies[9] or other combinations of two spectral components.[10] Magnetar soft X-ray emission is predominantly of thermal origin, but the emerging spectrum is more intricate than a simple Planckian (e.g., Refs. [10] and [11]). This is not surprising if we take into account the presence of the strongly magnetized atmosphere and the effects of the resonant cyclotron scattering within the magnetosphere of the magnetar.[12] Recently, observations from the Rossi X-Ray Timing Explorer and the International Gamma-Ray Astrophysics Laboratory have revealed that the magnetars are luminous persistent sources of 100 keV X-rays. These hard X-rays can be emitted only in the exterior of the magnetar, which illustrates the existence of an active plasma corona.[13]

We study in this work the mechanism for magnetar soft X-ray/γ-ray emission, where X-ray/γ-ray emission denotes the emission from X-ray to γ-ray. To explain the soft X-ray/γ-ray emission of a magnetar, various theories have been put forward, e.g., Refs. [14]–[17]. There are also some promising physical models that explain the absence of the cyclotron features and the hard X-ray tails.[18,19]

In the fall-back disk model, different mechanisms for the formation of the disk and the relation between the disk and the observed magnetar soft X-ray/γ-ray luminosity have been considered.[20−24] The enhanced X-ray emission and the expected optical/infrared flux from the magnetar can be successfully interpreted as due to the evolution of the disks after they have been pushed back by the bursts. The major disadvantage of this model is that it is unable to give a clear accounting for the bursts and the flares.[25]

In the twisting magnetosphere model, it is widely supposed that the energy caught in the twisting magnetic field gradually dissipates into X-rays. The gradual dissipation of the magnetospheric currents can generate the persistent soft γ-ray emission.[26] The persistent soft X-ray emission can be induced by the twisting of the external magnetic field caused by the motion of the star interior, while the persistent hard X-ray emission originates from a transition layer between the corona and the atmosphere.[27] However, this model is built upon the α–Ω dynamo model. So far there has been no observational indication for the existence of field $B \geq 10^{16}$ G inside an NS.

The thermal emission model has been studied extensively during the last ten years, and significant progresses have been made by many authors. However, some of the most fundamental questions in this model remain unanswered, for example, where the heat comes from.

So other possible mechanisms for the magnetar soft X-ray/γ-ray emission have to be studied. In this paper, we propose a possible mechanism for the magnetar soft X-ray/γ-ray emission. We focus on the interior of the magnetar, where the reaction of electron capture $e^-+p\rightarrow n+\nu_e$ occurs. The reaction of electron capture (EC), also known as inverse β decay, is a key physical step in nucleosynthesis and neutrino production in supernovae.[28−32] The EC sends away energy and entropy in the form of neutrinos, and reduces the number of electrons in the interior of the NS. Thus, the rate of EC has a significant impact on the origin and the evolution of the magnetic fields of the NS. The superhigh magnetic fields ($B \gg B_{\rm cr}$, $B_{\rm cr} = m_e^2c^3/e\hbar = 4.414\times 10^{13}$ G is called the quantum critical magnetic field, at which the cyclotron energy of an electron becomes comparable to its rest-mass energy) increase the electron Fermi energy $E_{\rm F}({\rm e})$,[33] which will induce the EC reaction inside the magnetar (mainly in the outer core). The high-energy neutrons created by the EC can easily destroy the anisotropic $^3P_2$ neutron Cooper pairs. This transition is accompanied by the release of magnetic energy. The released magnetic energy will be transformed into thermal energy. Only a very small part of this thermal energy is transported from the interior to the surface by conduction, and is converted into radiation as soft X-rays/γ-rays. Further details about this process is given in Section 3.

This paper is organized as follows. In Section 2, the energies of particles participating in the EC reaction are calculated. In Section 3, a brief review on the $^3P_2$ neutron Cooper pairs is presented, and a numerical simulation of the magnetar's cooling is carried out. In Section 4, an alternative explanation for the soft X/γ-ray emission of the magnetar is provided, and the luminosity $L_{\rm X}$ is calculated. The main conclusions are presented in Section 5.

2. Energies of particles and EC rates

2.1. Electron Fermi energy and energy state densities

We now consider the case with a superhigh magnetic field B directed along the z axis. The electrons are situated in disparate energy states in order from the lowest energy to the Fermi energy (the highest energy) with the Fermi momentum $p_{\rm F}({\rm e})$ (the highest momentum) along the magnetic field. In this case, the electron Fermi energy is determined by

$$\frac{4\pi g_0}{3B^*}\left(\frac{m_{\rm e}c}{h}\right)^3\left(\frac{E_{\rm F}({\rm e})}{m_{\rm e}c^2}\right)^4 I(t)=N_{\rm A}\rho Y_{\rm e}, \qquad (1)$$

where g_0 is the statistical weight of an energy level, which is dependent on the model used, in our model, we have assumed a uniform magnetic field, $g_0\equiv 1$, so it can be ignored in the following calculations; B^* is a dimensionless field defined as $B^*=B/B_{\rm cr}$; $I(t)$ denotes $\int_0^1(1-t^2)^{3/2}\,{\rm d}\,t$, $t=(p_z/m_{\rm e}c)/(E_{\rm F}({\rm e})/m_{\rm e}c^2)=p_zc/E_{\rm F}({\rm e})$; $N_{\rm A}=6.02\times10^{23}$ is Avogadro's constant; and $Y_{\rm e}$ is the the mean electron number per baryon. A special solution for Eq. (1) is

$$E_{\rm F}({\rm e})=60\left(\frac{Y_{\rm e}}{0.05}\frac{\rho}{\rho_0}\right)^{1/4}(B^*)^{1/4}\ ({\rm MeV}),$$
$$(\rho\sim(1-5)\times10^{14}\ ({\rm g\cdot cm^{-3}}),\ (B^*\geq1), \qquad (2)$$

where $\rho_0=2.8\times10^{14}$ g·cm^{-3} is the standard nuclear density.[33]

As soon as the energies of electrons near the Fermi surface (in momentum space) obviously exceed the threshold energy (Q) for the EC in the superhigh magnetic field, the EC reaction will dominate in the interior of the magnetar according to our assumptions.[4,34] For each species j in the empty space, we have

$$\rho_j\,{\rm d}\,E_j={\rm d}^3\,n_j=V_1\frac{{\rm d}^3\,p_j}{h^3}g_j, \qquad (3)$$

where V_1 denotes the normalization volume, n_j is the particle number of species j, ρ_j is the energy state density for species j (the particle number per unit energy), and g_j is the spin degeneracy for species j (g_j = 2 for fermions) (see Eq. (11.5.2) in Ref. [35]). In the vicinity of the Fermi surface, $E_j\sim E_{\rm F}(j)$ (j = e, p, n, ν). Since protons and neutrons are degenerate and non-relativistic, we obtain $E_{\rm p}\sim E'_{\rm F}({\rm p})=p_{\rm p}^2/2m_{\rm p}$ and $E_{\rm n}\sim E'_{\rm F}({\rm n})=p_{\rm n}^2/2m_{\rm n}$. Then we obtain ${\rm d}\,E_{\rm p}=p_{\rm p}\,{\rm d}\,p_{\rm p}/m_{\rm p}$ and ${\rm d}\,E_{\rm n}=p_{\rm n}\,{\rm d}\,p_{\rm n}/m_{\rm n}$, where $E'_{\rm F}({\rm n})$ and $E'_{\rm F}({\rm p})$ are the neutron Fermi kinetic energy and the proton Fermi kinetic energy, respectively.[35] Since

$$\rho_{\rm p}\,{\rm d}\,E_{\rm p}=2\times\frac{4\pi}{h^3}p_{\rm p}^2\,{\rm d}\,p_{\rm p}=\frac{8\sqrt{2}\pi}{h^3}m_{\rm p}^{3/2}E_{\rm p}^{1/2}\,{\rm d}\,E_{\rm p}$$

and

$$\rho_{\rm n}\,{\rm d}\,E_{\rm n}=2\times\frac{4\pi}{h^3}p_{\rm n}^2\,{\rm d}\,p_{\rm n}=\frac{8\sqrt{2}\pi}{h^3}m_{\rm n}^{3/2}E_{\rm n}^{1/2}\,{\rm d}\,E_{\rm n},$$

the energy state densities of neutrons and protons can be approximately expressed as

$$\rho_{\rm n}\simeq\frac{8\sqrt{2}\pi}{h^3}(m_{\rm n})^{3/2}E'_{\rm F}({\rm n})^{1/2}, \qquad (4)$$

and

$$\rho_{\rm p}\simeq\frac{8\sqrt{2}\pi}{h^3}(m_{\rm p})^{3/2}E'_{\rm F}({\rm p})^{1/2}, \qquad (5)$$

respectively.

In the light of the Pauli exclusion principle, the electron energy state number density $N_{\rm pha}$ should be equal to the electron number density $n_{\rm e}$. From Eq. (29) of Ref. [33], we obtain an approximate differential equation for the electron energy state density $\rho_{\rm e}$

$$\rho_{\rm e}\,{\rm d}\,E_{\rm e}\simeq\frac{4\pi}{3B^*}\left(\frac{m_{\rm e}c}{h}\right)^3\frac{1}{m_{\rm e}c^2}\times\left[\left(\frac{E_{\rm F}({\rm e})}{m_{\rm e}c^2}\right)^2-\left(\frac{E({\rm e})}{m_{\rm e}c^2}\right)^2\right]^{3/2}{\rm d}\,E_{\rm e}. \qquad (6)$$

Simplifying Eq. (6) gives

$$\rho_{\rm e}\simeq\frac{4}{3}\frac{\pi}{B^*}\left(\frac{m_{\rm e}c}{h}\right)^3\frac{1}{m_{\rm e}c^2}\times\left[\left(\frac{E_{\rm F}({\rm e})}{m_{\rm e}c^2}\right)^2-\left(\frac{E({\rm e})}{m_{\rm e}c^2}\right)^2\right]^{3/2}. \qquad (7)$$

Since neutrinos are degenerate, relativistic, and massless, by using energy conservation $E_\nu=E_{\rm e}-Q=p_\nu c$, we also obtain an expression for the neutrino energy state density ρ_ν

$$\rho_\nu=\frac{(E_{\rm e}-Q)^2}{2\pi^2\hbar^3c^3}, \qquad (8)$$

where p_ν is the neutrino momentum.

2.2. Energies of particles and EC rates

We concentrate on the non-relativistic, degenerate nuclear matter and the ultra-relativistic, degenerate electrons. The β equilibrium implies the following relationship among the chemical potentials (called the Fermi energies $E_{\rm F}$) of particles: $\mu_{\rm p}+\mu_{\rm e}=\mu_{\rm n}$, where the neutrino chemical potential is ignored. In

the case of $0.5\rho_0 \leq \rho \leq 2\rho_0$, the following expressions hold approximately (see Chap. 11 of Ref. [35]): $E'_{\rm F}({\rm n}) = 60(\rho/\rho_0)^{2/3}$ MeV, $E'_{\rm F}({\rm p}) = 1.9(\rho/\rho_0)^{\frac{4}{3}}$ MeV, and $(m_{\rm n} - m_{\rm p})c^2 = 1.29$ MeV. For convenience, we set $\rho = \rho_0$ and $Y_{\rm e} = 0.05$ in all the following calculations. This setting yields $Q = E_{\rm F}({\rm n}) - E_{\rm F}({\rm p}) = (m_{\rm n}-m_{\rm p})c^2+(p^2_{\rm F}({\rm n})/2m_{\rm n}-p^2_{\rm F}({\rm p})/2m_{\rm p}) = 59.39$ MeV. Therefore, the range of $E_{\rm e}$ is $Q \sim E_{\rm F}({\rm e})$. For the outgoing EC neutrons, their kinetic energies $E_{\rm k}({\rm n})$ cannot be less than the neutron Fermi kinetic energy ($E'_{\rm F}({\rm n}) = 60$ MeV), otherwise the process of EC will not occur. Thus, the range of $E_{\rm k}({\rm n})$ is assumed to be $E'_{\rm F}({\rm n}) \sim \langle E_{\rm n}\rangle$. By employing energy conservation $E_{\rm e}+E_{\rm p} = E_{\rm n}+E_\nu$, we can calculate the Fermi energy of the neutrinos produced by the EC as

$$E_{\rm F}(\nu) = E_{\rm F}({\rm e}) - Q = E_{\rm F}({\rm e}) - 59.39 \text{ MeV}. \quad (9)$$

The EC rate Γ is defined as the number of electrons captured by one proton per second, and can be calculated using the standard charged-current β-decay theory. The expression for ${\rm d}\,\Gamma$ reads

$$\begin{aligned}{\rm d}\,\Gamma = {} & \frac{(kT)^4\exp(-\Delta_{\max}(^3{\rm P}_2)/kT)}{E'_{\rm F}({\rm n})E'_{\rm F}({\rm p})E_{\rm F}({\rm e})E_{\rm F}(\nu_{\rm e})}\frac{2\pi}{\hbar} \\ & \times G^2_{\rm F}C^2_{\rm V}(1+3a^2)S\rho_\nu\,{\rm d}\,E_\nu\delta(E_\nu+Q-E_{\rm e}),\end{aligned} \quad (10)$$

where $k = 1.38\times10^{-16}$ erg·K^{-1} is the Boltzmann constant; $G_{\rm F} = 1.4358\times10^{-49}$ erg·cm^3 is the universal Fermi coupling constant in the Weinberg–Salam–Glashow theory; $C_{\rm V} = 0.97374$ is the vector coupling constant; and a is the ratio of the coupling constant of the axial vector weak interaction constant to that of the vector weak interaction constant, $a = 1.253$ in experiments. And $S = f_{\rm e}f_{\rm p}(1-f_{\rm n})(1-f_\nu)$, where quantity $(1-f_j)$ is called the blocking factor, which represents the fraction of the unoccupied phase space for the j-th species of particles. For fermions, e.g., electrons, protons, neutrons, and neutrinos/antineutrinos, we assume the Fermi–Dirac equilibrium distributions

$$f(j) = \frac{1}{\exp[(E_j-\mu_j)/kT)]+1}. \quad (11)$$

In the interior of the NS, for electrons, $f_{\rm e} = 1$ when $E_{\rm e} < E_{\rm F}({\rm e})$, and $f_{\rm e} = 0$ when $E_{\rm e} > E_{\rm F}({\rm e})$; for protons, $f_{\rm p} = 1$ when $E_{\rm p} < E'_{\rm F}({\rm p})$, and $f_{\rm p} = 0$ when $E_{\rm p} > E'_{\rm F}({\rm p})$; for neutrons, $(1-f_{\rm n}) = 0$ when $E_{\rm k}({\rm n}) < E'_{\rm F}({\rm n})$, and $(1-f_{\rm n}) = 1$ when $E_{\rm k}({\rm n}) > E'_{\rm F}({\rm n})$; for neutrinos, $(1-f_\nu) = 1$. It follows that factor $S = f_{\rm e}f_{\rm p}(1-f_{\rm n})(1-f_\nu) \simeq 1$ can be ignored in the following calculations.

In Eq. (10), the fourth power of kT originates due to the following reason. The reaction $e^- + p \leftrightarrow n + \nu_{\rm e}$ in equilibrium gives ${\rm d}\,Y_{\rm e} = {\rm d}\,Y_{\rm p} = -{\rm d}\,Y_{\rm n} = -{\rm d}\,Y_{\nu_{\rm e}}$, where Y_j is the concentration of the j-th species of particles. For each degenerate species, only a fraction $\sim kT/E_{\rm F}(j)$ of particles can effectively contribute to Γ. Thus, the term of $(kT)^4$ must be included in Eq. (10).

As we know, the neutrons are universally locked in a superfluid state in the NS. The neutron superfluid restrains all reactions (including β decay and inverse β decay) occurring inside the NS obviously, so the value of Γ is reduced by a factor of $\sim\exp(-\Delta_{\max}(^3{\rm P}_2)/kT)$, where $\Delta_{\max}(^3{\rm P}_2) \sim 0.048$ MeV is the maximal binding energy (or the maximal energy gap) of the $^3{\rm P}_2$ neutron Cooper pair (see Section 3.1 for details). For convenience, we define

$$\Lambda = \frac{(kT)^4\exp(-\Delta_{\max}(^3{\rm P}_2)/kT)}{E'_{\rm F}({\rm n})E'_{\rm F}({\rm p})E_{\rm F}({\rm e})E_{\rm F}(\nu_{\rm e})}, \quad (12)$$

where Λ is called the Landau level superfluid modified factor. To find the total electron capture rate per proton, we integrate over all initial electron states and E_ν. Inserting Eqs. (7) and (8) into Eq. (10) gives

$$\begin{aligned}\Gamma = {} & \frac{(kT)^4\exp(-\Delta_{\max}(^3{\rm P}_2)/kT)}{E'_{\rm F}({\rm n})E'_{\rm F}({\rm p})E_{\rm F}({\rm e})E_{\rm F}(\nu_{\rm e})} \\ & \times\frac{G^2_{\rm F}C^2_{\rm V}(1+3a^2)}{\pi\hbar^4c^3}\frac{4\pi}{3B^*}\left(\frac{m_{\rm e}c}{h}\right)^3\frac{1}{(m_{\rm e}c^2)^4} \\ & \times\int_Q^{E_{\rm F}({\rm e})}E^2_\nu\,{\rm d}\,E_\nu f_{\rm e}f_{\rm p}(1-f_{\rm n})(1-f_\nu) \\ & \times[E^2_{\rm F}({\rm e})-E^2({\rm e})]^{3/2}\,{\rm d}\,E_{\rm e}\delta(E_\nu+Q-E_{\rm e}) \\ \simeq {} & \Lambda\frac{G^2_{\rm F}C^2_{\rm V}(1+3a^2)}{\pi\hbar^4c^3}\frac{4\pi}{3B^*}\left(\frac{m_{\rm e}c}{h}\right)^3\frac{1}{(m_{\rm e}c^2)^4} \\ & \times\int_Q^{E_{\rm F}({\rm e})}[E^2_{\rm F}({\rm e})-E^2({\rm e})]^{3/2}(E_{\rm e}-Q)^2\,{\rm d}\,E_{\rm e}.\end{aligned} \quad (13)$$

To determine the value of $L_{\rm X}$ in the superhigh magnetic field, we must first calculate $E_{\rm F}({\rm e})$, $E_{\rm F}(\nu)$, $\langle E_{\rm n}\rangle$, and $\langle E_\nu\rangle$, where $\langle E_{\rm n}\rangle$ and $\langle E_\nu\rangle$ are the average kinetic energies of the outgoing neutrons and neutrinos, respectively. And $\langle E_\nu\rangle$ and $\langle E_{\rm n}\rangle$ are determined by

$$\begin{aligned}\langle E_\nu\rangle = \int E_\nu\,{\rm d}\,\Gamma/\Gamma = {} & \int_Q^{E_{\rm F}({\rm e})}[E^2_{\rm F}({\rm e})-E^2({\rm e})]^{3/2} \\ & \times(E_{\rm e}-Q)^3\,{\rm d}\,E_{\rm e}/I,\end{aligned} \quad (14)$$

and

$$\langle E_{\rm n}\rangle = E_{\rm F}({\rm e}) - \langle E_\nu\rangle + 0.61 \text{ MeV}, \quad (15)$$

respectively, where $I = \int_Q^{E_{\rm F}({\rm e})}[E^2_{\rm F}({\rm e})-E^2({\rm e})]^{\frac{3}{2}}(E_{\rm e}-Q)^2\,{\rm d}\,E_{\rm e}$. The calculation results are partly shown in Table 1.

Table 1. Calculation results of related energies.

$B/10^{14}$ G	$E_{\rm F}$(e)/MeV	$E_{\rm F}(\nu)$/MeV	$\langle E_\nu\rangle$/MeV	$\langle E_{\rm n}\rangle$/MeV
1.0	73.61	14.22	10.98	63.24
2.0	87.54	28.15	22.15	66.01
3.0	96.88	37.49	29.77	67.72
4.0	104.10	44.71	35.72	68.99
6.0	115.21	55.82	44.95	70.87
8.0	123.80	64.41	52.12	72.29
10	130.90	71.51	58.07	73.44
15	144.87	85.48	69.83	75.65
20	155.67	96.28	78.94	77.34
25	164.60	105.21	86.60	78.71
30	172.28	112.89	93.01	79.88

3. Numerically simulating magnetar cooling and magnetic field decay

3.1. The $^3P_2$ Cooper pairs and superhigh magnetic fields

As we know, the formation of Cooper pairs is a universal quantum-mechanical condensation phenomenon found in superfluids or superconductors. In 1956, Bardeen, Cooper, and Schrieffer first pointed out that the pairing occurs basically between fermions near the Fermi surface, and the most favorable situation occurs when the two fermions' spins are equal and opposite, since the matrix elements are the largest in this case.[36]

Owing to the pairing correlations, there is a major change in the low-energy spectrum of the system. A finite energy gap between its ground state and the first excited state appears, and then the system will be subjected to a phase transition to a superfluid (or superconductor) state below a critical temperature $T_{\rm c}$. The magnitude of the pairing correlation length (or dimension) is hundreds of fm, which is much larger than the mean separation of neutrons (the mean separation distance of nucleons is ∼1 fm inside the NS).

In the previous papers, e.g., Refs. [37] and [38], those authors have studied the $^3P_2$ state for neutrons, and found that the $^3P_2$ energy gap $\Delta(^3P_2)$ has a maximum of ∼ 0.12–0.13 MeV for the pure neutron matter. In 1996, Elgary and his collaborators took the conditions for the β equilibrium into account. Based on a realistic NS model (i.e., the non-pure neutron matter model),[39,40] they found that the $^3P_2$ energy gap appears in the region of 1.32 fm^{-1} $< k_{\rm F} <$ 2.34 fm^{-1} and the maximum of $\Delta(^3P_2)$ is about 0.05 MeV (see Fig. 1).

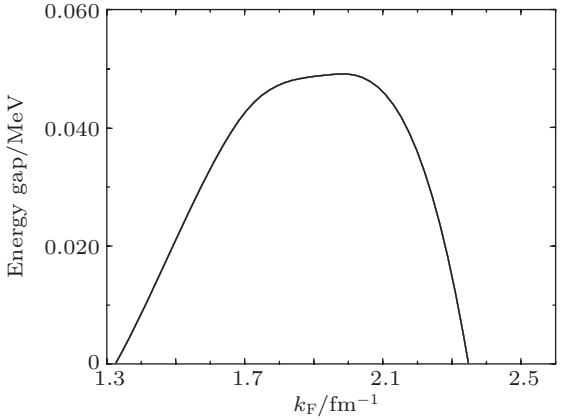


Fig. 1. Neutron energy gap for the $^3P_2$ partial wave in the β equilibrium. This figure is cited from Ref. [37], where $k_{\rm F}$ is the neutron Fermi wave number.

We have recently found that[4] the maximum of $\Delta(^3P_2)$ is about 0.048 MeV at $k_{\rm F} = 1.96$ fm^{-1}, and $\Delta(^3P_2)$ is almost a constant in the rather wide range of 1.8 fm^{-1} $< k_{\rm F} <$ 2.1 fm^{-1} (with the maximal error less than 3%) corresponding to the density region of 3.3×10^{14} g· cm^{-3} $< \rho < 5.2 \times 10^{14}$ g·cm^{-3}. Moreover, the critical temperature, which is also called the Curie temperature of the $^3P_2$ neutron Cooper pairs, is calculated as $T_{\rm cn} = \Delta_{\rm max}(^3P_2)/2k \approx 2.78 \times 10^8$ K. Thus, based on our assumptions,[4,6,7] the maximal internal temperature $T_{\rm in}$ (not including the inner core temperature) cannot exceed $T_{\rm cn}$.

The system of the $^3P_2$ Cooper pairs with spin $s = 1$ may be regarded as a Bose–Einstein system. All the $^3P_2$ Cooper pairs may condense into the same state with the lowest energy (the ground state) at a moderately low temperature ($T \ll T_{\rm cn}$). Such a system is also stable as long as $T \ll T_{\rm cn}$, unless it is

subjected to a severe disturbance, e.g., thermal excitation, high-energy particle flux, and so on.

An external magnetic field tends to align the magnetic moments in the direction of the applied field, because a paramagnetic magnetic moment possesses lower energy than a diamagnetic magnetic moment under an external magnetic field, whereas the thermal motion tends to randomize the directions of the magnetic moments. Therefore, the lower the temperature is, the stronger the paramagnetic field is. The paramagnetic field produced by the aligned magnetic moments reinforces the external field.

The magnetars/SNRs associations confirm that the magnetars originate from the core-collapse supernovae. The magnetar progenitor cools quickly via the neutrino emission from its core, which causes the star's internal temperature to fall sharply,[6,7,10,41] and a paramagnetic transition will occur when the internal temperature drops to the critical temperature.[6,7] The superhigh magnetic fields of the magnetars may originate from the paramagnetic fields produced by the aligned magnetic moments of the $^3P_2$ Cooper pairs below their critical (or transition) temperature, and the maximal paramagnetic field is about (3.0–4.0)$\times 10^{15}$ G.[6,7]

3.2. Numerical simulation

The initial conditions (e.g., B, T) of the magnetars are likely to be very different, implying that their values of Λ are also different. In order to numerically simulate the magnetar cooling and the magnetic field decay, for convenience, we assume a uniform initial magnetic field $B_0 = 3.0 \times 10^{15}$ G. Since the maximum initial temperature cannot exceed $T_{\rm cn}$, we can assume $T_{\rm in}(0)$ to be 2.60×10^8 K, 2.40×10^8 K, 2.20×10^8 K, 2.00×10^8 K, and 1.80×10^8 K, respectively.

In the interior of a magnetar, the β decay and the inverse β decay occur simultaneously as required by the charge neutrality. So when B decays, the depleted protons and electrons are recruited many times, which leads to only a small decrease in $Y_{\rm e}$ and $Y_{\rm p}$. In addition, the electrons are super-relativistic and degenerate, when the internal temperature falls, the electron transition between Landau levels is not permitted, because the electrons can be approximately treated as a zero-temperature Fermi gas. Therefore, the value of Λ changes very little, and can be considered as a constant in a rather short timescale (or the magnetar lifetime).[2,3] Holding the value of Λ unchanged, we numerically simulate the processes of magnetar cooling and magnetic field decay. The main results are partly shown in Table 2.

Table 2. Numerically simulated magnetar cooling and magnetic field decay. The temperature is in the unit of 10^8 K.

$B/10^{14}$ G	T^1	T^2	T^3	T^4	T^5	T^6
30	2.60	2.40	2.20	2.00	1.80	1.60
25	2.55	2.35	2.16	1.96	1.77	1.57
20	2.49	2.30	2.11	1.92	1.73	1.54
15	2.42	2.24	2.05	1.87	1.69	1.51
10	2.31	2.14	1.97	1.80	1.63	1.45
8.0	2.26	2.09	1.93	1.76	1.59	1.42
6.0	2.18	2.03	1.87	1.71	1.55	1.37
4.0	2.08	1.93	1.78	1.63	1.48	1.33
3.0	2.00	1.86	1.72	1.58	1.44	1.29
2.0	1.89	1.76	1.63	1.50	1.37	1.23
1.0	1.68	1.57	1.46	1.38	1.23	1.12

In Table 2, the values of Λ are 1.34 $\times 10^{-14}$, 8.15 $\times 10^{-15}$, 4.66 $\times 10^{-15}$, 2.47 $\times 10^{-15}$, 1.19 $\times 10^{-15}$, and 5.05 $\times 10^{-16}$ for columns 2, 3, 4, 5, 6, and 7, respectively. In order to maximally reduce the influence of the accidental error on the later calculations, we also compute the average value of Λ, $\langle \Lambda \rangle \simeq 5.02 \times 10^{-15}$, which will be used in later calculations.

4. Soft X-ray luminosities of magnetars

4.1. Physics of magnetar soft X/γ-ray emission

In this part, we provide a possible mechanism for the magnetar's soft X-ray/γ-ray emission as follows.

(i) As discussed in Section 3.1, the superhigh magnetic fields of magnetars may originate from the paramagnetic fields produced by the aligned magnetic moments of the $^3P_2$ Cooper pairs below their transition temperature. After being paramagnetized, each $^3P_2$ neutron Cooper pair has magnetic energy $2\mu_{\rm n}B$ in the applied magnetic field due to its magnetic moment $2\mu_{\rm n}$ in the anisotropic neutron superfluid, where $\mu_{\rm n}$=0.966 $\times 10^{-23}$ erg·G^{-1} is the neutron abnormal magnetic moment.

(ii) When ρ and $Y_{\rm e}$ are given, the Fermi energy of electrons inside the magnetar is nearly proportional to $\frac{1}{4}$ power of the magnetic field strength B, i.e., $E_{\rm F}({\rm e}) \propto B^{1/4}$. It is very likely that $E_{\rm F}({\rm e})$ is higher than both the neutron Fermi kinetic energy

$E'_{\rm F}({\rm n})$ and the threshold energy of the inverse β decay in superhigh magnetic field Q (in the case of $\rho = \rho_0$ and $Y_{\rm e} = 0.05$, $E'_{\rm F}({\rm n})$= 60 MeV, Q = 59.39 MeV, so $E'_{\rm F}({\rm n}) \simeq Q$).

(iii) If the energies of electrons inside a magnetar obviously exceed Q, a part of protons near the (proton) Fermi surface (in momentum space) will spontaneously capture electrons lying in the vicinity of the (electron) Fermi surface. Since the kinetic energies of outgoing EC neutrons are higher than $E'_{\rm F}({\rm n})$, the EC reaction is permitted, without being hindered by the Pauli exclusion principle. However, the outgoing EC neutrons cannot escape from the star due to the superhigh density of the internal matter.

(iv) Most of the energy lost during the process of EC is carried away by neutrinos. Only a small fraction of this energy can effectively heat the internal matter. Since the maximum binding energy of the $^3{\rm P}_2$ neutron Cooper pair is only about 0.048 MeV, the outgoing EC neutrons with high kinetic energies can easily destroy the $^3{\rm P}_2$ Cooper pairs through the interaction of nuclear force. This reaction can be expressed as ${\rm n} + ({\rm n}\uparrow {\rm n}\uparrow) \longrightarrow {\rm n} + {\rm n} + {\rm n}$. The energies required to destroy the $^3{\rm P}_2$ Cooper pairs are provided by the kinetic energies of these outgoing EC neutrons.

(v) When being destroyed by a high-energy EC neutron, the magnetic moment of a $^3{\rm P}_2$ neutron Cooper pair is no longer arranged in the paramagnetic direction, and the magnetic energy ($2\mu_n B$) is released. Then the superhigh magnetic field produced by the aligned magnetic moments of the $^3{\rm P}_2$ Cooper pairs will disappear gradually. The magnetic energy released will be converted into the thermal energy. While accumulating to a certain degree, a portion of the thermal energy converted will be transported from the star interior to the star surface by heat conduction. At the surface, it is converted into surface thermal emission, because $kT \sim 2\mu_{\rm n}B \sim 10B_{15}$ keV, where B_{15} is the magnetic field in units of 10^{15} G. However, the overwhelming majority of the heat transported to the surface is carried away by the surface neutrino emission. Only a small fraction can be converted into soft X-rays/γ-rays. After a highly efficient modulation within the magnetar magnetosphere, the thermal surface emission is shaped into a spectrum with the observed characteristics of the magnetars. Notice that the luminosity $L_{\rm X}$ is ultimately determined by the magnetic field.

(vi) Due to the absorption by the star's inner matter and the neutrino emission, most thermal energy converted is lost before it reaches the surface. The absorbed thermal energy may maintain a relative thermodynamic equilibrium in the interior of the magnetar. Since there exist neutrino coherent scatterings from electrons (protons) and neutrons, the highest energies of neutrinos escaping from the star interior could be as high as several MeV. The total heat carried away by neutrinos could be slightly larger than that absorbed despite of the compactness of the inner matter. Therefore, the whole process of EC can be seen as a long-term inner cooling process accompanied by the magnetic field decay.

The soft X-ray/γ-ray flux of the magnetar, in short, is thermal in nature, and the value of $L_{\rm X}$ is ultimately determined by the magnetic field B. However, we must stress that $L_{\rm X}$ is only a weak function of the internal temperature. The internal temperature is only equivalent to the background temperature, and decreases with decreasing B, whereas the surface temperature controlled by the crustal physics is largely independent of the core's evolution.

4.2. Preliminary values of $L_{\rm X}$ of magnetars

Investigations of magnetars suggest that the magnetic fields could be the ultimate energy source for all the observed surface emissions of the magnetars, e.g. Refs. [1]–[3], and [10]. The effects of the superhigh magnetic fields would be to speed up the magnetar cooling. Before calculating $L_{\rm X}$ of the magnetar, let us consider the following hypothetical case. We assume that all $^3{\rm P}_2$ neutron Cooper pairs are destroyed, the total magnetic energy released can be estimated by

$$E \simeq 2\mu_{\rm n}B \times \frac{qN_{\rm A}m(^3{\rm P}_2)}{2} \simeq 4.4\times 10^{47}\frac{m(^3{\rm P}_2)}{0.1M_{\rm sun}}\ ({\rm erg}), \qquad (16)$$

where $B \sim 3.0\times 10^{15}$ G, and $q \sim 8.7\%$ is the fraction of neutrons that are combined into $^3{\rm P}_2$ neutron Cooper pairs.[6] If this energy is totally transformed into thermal energy, and if the observed persistent soft X-ray flux from the magnetar is powered by the thermal energy transformed (without consideration of the energy loss), then the magnetar may maintain a mean luminosity $\langle L_{\rm X}\rangle \sim 1.0\times(10^{33}$–$10^{35})$ erg·s $^{-1}$ over a period of $t \sim 1.4\times(10^7$–$10^5)$ a. Such a period will be far longer than the ages of any supernova remnants (SNRs) associated with the magnetars ($t_{\rm SNR}$ is

about several thousand years for any known magnetars' SNRs, e.g., Refs. [10] and [41]).

Now, let us estimate the probability that an outgoing EC neutron destroys one $^3P_2$ Cooper pair. The number of neutrons participating in the EC per unit volume $n'_{\rm n}$ is calculated as

$$n'_{\rm n} = \frac{kT}{E'_{\rm F}({\rm n})}\int \rho_{\rm n}\,{\rm d}\,E_{\rm n} = \frac{kT}{E'_{\rm F}({\rm n})}\times\frac{8\pi\sqrt{2}m_{\rm n}^{3/2}}{h^3}\int_{E'_{\rm F}({\rm n})}^{\langle E_{\rm n}\rangle} E_{\rm n}^{1/2}\,{\rm d}\,E_{\rm n}. \quad (17)$$

As an example, we can arbitrarily assume $B = 3.0\times 10^{15}$ G and $T = 2.78\times 10^8$ K. Inserting these two quantites (B and T) into Eq. (17) simultaneously, we estimate $n'_{\rm n} = 4.47\times 10^{34}$ cm^{-3} ($\rho = \rho_0$). Since the assumed values of these two qualities are the maximum values of B and T, the average value of $n'_{\rm n}$ is obviously less than the value of $n'_{\rm n}$ evaluated above. In the interior of an NS, where the anisotropic $^3P_2$ neutron superfluid exists, the neutron number density is $n_{\rm n} = 1.78\times 10^{38}$ cm^{-3} ($\rho = \rho_0$),[35] which shows that both the number of neutrons and the number of $^3P_2$ neutron Cooper pairs per unit volume are far larger than the number of these newly formed EC neutrons per unit volume. Based on the above estimation and analysis, we may make a reasonable assumption that each outgoing high-energy EC neutron can destroy one $^3P_2$ neutron Cooper pair. Accordingly, the magnetic energy release rate in the interior of the magnetar can be computed as

$$\frac{{\rm d}\,E_{\rm B}}{{\rm d}\,t} \simeq \frac{(kT)^4\exp(-\Delta_{\max}(^3{\rm P}_2)/kT)}{E'_{\rm F}({\rm n})E'_{\rm F}({\rm p})E_{\rm F}({\rm e})E_{\rm F}(\nu_{\rm e})}V(^3{\rm P}_2) \times\frac{(2\pi)^4}{\hbar V_1}G_{\rm F}^2C_{\rm V}^2(1+3a^2) \times\int {\rm d}^3\,n_{\rm e}\,{\rm d}^3\,n_{\rm p}\,{\rm d}^3\,n_{\rm n}\,{\rm d}^3\,n_\nu\delta(E_\nu+Q-E_{\rm e}) \times\delta^3(\boldsymbol{K}_{\rm f}-\boldsymbol{K}_{\rm i})S\Delta E(^3{\rm P}_2), \quad (18)$$

where $V(^3{\rm P}_2)\sim\frac{4}{3}\pi R_5^3$ is the volume of the anisotropic $^3P_2$ neutron superfluid, V_1 is the normalized volume, and $\Delta E(^3{\rm P}_2) = 2\mu_{\rm n}B$ is the element of the magnetic energy released.

According to our model, the observed soft X-ray/γ-ray output of the magnetar is dominated by the transportation of the magnetic energy through the core. For the purpose of calculating $L_{\rm X}$, we must introduce another important parameter ζ, the overall soft X-ray efficiency coefficient of the magnetar. The main reasons for introducing ζ are presented as follows.

i) The overwhelming majority of the thermal energy converted will be lost due to the absorption by the star's inner matter and the neutrino emission during the process of heat conduction. Thus, we introduce a thermal energy transfer coefficient θ defined as the ratio of the net thermal energy transported to the star's surface to the total thermal energy converted from the magnetic energy.

ii) In the same way, the thermal energy conducted to the surface is incapable of being entirely converted into electromagnetic radiation due to the energy loss (mainly via the neutrino emission). So we also introduce an energy conversion efficiency ϵ defined as the ratio of the soft X-ray radiation energy emitted to the thermal energy transported to the star surface by heat conduction.

iii) The heat conduction is one of the most important characteristics of matter, Chinese scientists have made significant progress in this field recently (e.g., Refs. [42]–[48]). However, owing to special circumstances (high temperatures, high-density matter, ultra-strong fields, and so on) inside a magnetar, so far the physics community has not directly determined the values of ϵ and θ. We define the overal soft X-ray efficiency coefficient of a magnetar as $\zeta = \epsilon\theta$. The average value of ζ may be estimated by comparing our calculations with magnetar observations.

Using the value of $\langle\zeta\rangle$, we calculate the luminosity $L_{\rm X}$ of the magnetar as

$$L_{\rm X} = \langle\zeta\rangle\frac{{\rm d}\,E_{\rm B}}{{\rm d}\,t}. \quad (19)$$

Inserting $\rho_j\,{\rm d}\,E_j = {\rm d}^3\,n_j$ and

$$\delta^3(\boldsymbol{K}_{\rm f}-\boldsymbol{K}_{\rm i})\,{\rm d}^3\,n_{\rm p}(2\pi)^3/V_1 = \delta^3(\boldsymbol{P}_{\rm f}-\boldsymbol{P}_{\rm i})\,{\rm d}^3\,P_{\rm p}$$

into Eq. (19) gives

$$L_{\rm X} \simeq \langle\Lambda\rangle\langle\zeta\rangle 2\mu_{\rm n}BV(^3{\rm P}_2)\frac{2\pi}{\hbar}G_{\rm F}^2C_{\rm V}^2(1+3a^2) \times\int\rho_{\rm e}\,{\rm d}\,E_{\rm e}\int\delta^3(\boldsymbol{P}_{\rm f}-\boldsymbol{P}_{\rm i})\,{\rm d}^3\,P_{\rm p}\int\rho_{\rm n}\,{\rm d}\,E_{\rm n} \times\int\delta(E_\nu+Q-E_{\rm e})\rho_\nu\,{\rm d}\,E_\nu. \quad (20)$$

Eliminating the δ-functions and simplifying Eq. (20) give

$$L_{\rm X} = \langle\Lambda\rangle\langle\zeta\rangle 2\mu_{\rm n}BV(^3{\rm P}_2)\frac{2\pi}{\hbar}G_{\rm F}^2C_{\rm V}^2(1+3a^2) \times\int_{E'_{\rm F}({\rm n})}^{\langle E_{\rm n}\rangle}\rho_{\rm n}\,{\rm d}\,E_{\rm n}\int_Q^{E_{\rm F}({\rm e})}(E_{\rm e}-Q)^2\rho_{\rm e}\,{\rm d}\,E_{\rm e}, \quad (21)$$

where $E'_{\rm F}({\rm n})\simeq 60$ MeV. Inserting Eqs. (4)–(7) into Eq. (21) gives a general formula for $L_{\rm X}$

$$L_{\rm X} \simeq \langle\Lambda\rangle\langle\zeta\rangle 2\mu_{\rm n}B\frac{4}{3}\pi R_5^3\frac{1}{\pi\hbar^4c^3}G_{\rm F}^2C_{\rm V}^2(1+3a^2) \times\frac{8\pi\sqrt{2}m_{\rm n}^{3/2}}{h^3}\frac{4\pi}{3B^*}\left(\frac{m_{\rm e}c}{h}\right)^3 \times\frac{(1.60\times10^{-6})^{7.5}}{(m_{\rm e}c^2)^4}\int_{60}^{\langle E_{\rm n}\rangle}E_{\rm n}^{1/2}\,{\rm d}\,E_{\rm n} \times\int_{Q}^{E_{\rm F}({\rm e})}[E_{\rm F}^2({\rm e})-E^2({\rm e})]^{3/2}(E_{\rm e}-Q)^2\,{\rm d}\,E_{\rm e}, \quad (22)$$

where the relation 1 MeV=1.60 $\times10^{-6}$ erg is used. Equation (22) gives the value of $L_{\rm X}$ as a function of B. The calculation results are partly shown in Table 3.

Table 3. Preliminary values of $L_{\rm X}$ of magnetars.

$B/10^{14}$ G	$E_{\rm F}({\rm e})$/MeV	$\langle E_{\rm n}\rangle$/MeV	$L_{\rm X}$/erg·s^{-1}
1.0	73.61	63.24	$9.530\times10^{33}\langle\zeta\rangle$
2.0	87.54	66.01	$4.783\times10^{35}\langle\zeta\rangle$
3.0	96.88	67.72	$2.552\times10^{36}\langle\zeta\rangle$
4.0	104.10	68.99	$7.233\times10^{36}\langle\zeta\rangle$
6.0	115.21	70.87	$2.727\times10^{37}\langle\zeta\rangle$
8.0	123.80	72.29	$6.487\times10^{37}\langle\zeta\rangle$
10	130.90	73.44	$1.228\times10^{38}\langle\zeta\rangle$
15	144.87	75.65	$3.683\times10^{38}\langle\zeta\rangle$
20	155.67	77.34	$7.726\times10^{38}\langle\zeta\rangle$
25	164.60	78.71	$1.347\times10^{39}\langle\zeta\rangle$
30	174.28	79.88	$2.099\times10^{39}\langle\zeta\rangle$

In order to determine the value of $\langle\zeta\rangle$, we must compare our calculations with the observed persistent parameters of the magnetars. The details are given in the next subsection.

4.3. Observation results

So far, there are 11 soft gamma repeater (SGR) candidates (7 confirmed) and 12 anomalous X-ray pulsar (AXP) candidates (9 confirmed). All known magnetars are X-ray pulsars with luminosities $L_{\rm X}\sim(10^{32}$–$10^{36})$ erg·s^{-1}. These fluxes are usually much higher than the rate at which the star loses its rotational energy, e.g., Refs. [3], [10], [16], [49]. In Table 4, we list the parameters determined form the observations for the confirmed magnetar candidates.

Table 4. Observational parameters of confirmed magnetars.

Name	P/s	$\dot{P}/10^{-11}$s·s^{-1}	$B^b/10^{14}$ G	$L_{\rm X}$/erg·s^{-1}	$({\rm d}\,E/{\rm d}\,t^c)$/erg·s^{-1}
SGR 0526-66	8.0544	3.8	5.6	1.4×10^{35}	2.9×10^{33}
SGR 1806-20	7.6022	75	24	$5.0^a\times10^{36}$	6.7×10^{34}
SGR 1900+14	5.1998	9.2	7.0	1.3×10^{35}	2.6×10^{34}
SGR 1627-41	2.5946	1.9	2.2	2.5×10^{33}	4.3×10^{34}
SGR 0501+4516	5.7621	0.58	1.9	–	1.2×10^{33}
SGR 0418+5729	9.0784	<0.0006	<0.075	–	$<3.2\times10^{29}$
SGR 1833+0832	7.5654	0.439	1.8	–	4.0×10^{32}
CXOUJ 0100	8.0203	1.88	3.9	7.8×10^{34}	1.4×10^{33}
1E 2259+586	6.9789	0.048	0.59	1.8×10^{35}	5.6×10^{31}
4U 0142+61	8.6883	0.196	1.3	$>5.3\times10^{34}$	1.2×10^{32}
1E 1841-045	11.7751	4.155	7.1	2.2×10^{35}	9.9×10^{32}
1RXSJ 1708	10.9990	1.945	4.7	1.9×10^{35}	5.7×10^{32}
CXO$^{\rm t}$J1647	10.6107	0.24	1.6	2.6×10^{34}	7.8×10^{31}
1E$^{\rm t}$1547.0-5408	2.0698	2.318	2.2	5.8×10^{32}	1.0×10^{35}
XTE$^{\rm t}$J1810-197	5.5404	0.777	2.1	1.9×10^{32}	1.8×10^{33}
1E$^{\rm d}$1048.1-5937	6.4521	2.70	4.2	5.4×10^{33}	3.9×10^{33}

All data are taken from the McGill AXP/SGR online catalog of 10 August 2011 (http://www.physics.mcgill.ca/~pulsar/magnetar/main.html) except for $L_{\rm X}$ of SGR 1806-20. The sign a denotes data from Thompson & Duncan (1996).[50] The sign b denotes the surface dipolar magnetic field of a pulsar estimated using its spin period P and spin-down rate $\dot{P}$, i.e., $B \simeq 3.2 \times 10^{19}(P\dot{P})^{\frac{1}{2}}$ G. The sign c denotes that a pulsar slows down with time as its rotational energy is lost via the magnetic dipolar radiation, and the loss rate is denoted as $\mathrm{d}E/\mathrm{d}t$. The signs d and t denote dim and transient AXPs, respectively.

Clearly, magnetars SGR 0501+4516, SGR 0418+5729, and SGR 1833+0832 with no persistent flux do not need to be considered essentially. In the light of our model, the persistent soft X-ray luminosity of a canonic magnetar should not be less than its rotational energy loss rate $\mathrm{d}E/\mathrm{d}t$. Therefore, we also do not need to take into account magnetars SGR 1627-41, 1E 1547.0-5408, and XTE J1810-197 in the following calculation of $\langle\zeta\rangle$.

Combining Eq. (21) with Table 4 gives the values of ζ for the confirmed magnetar candidates. Table 5 shows the calculation results.

Table 5. Calculation results of ζ of confirmed magnetars.

Name	$B/10^{14}$ G	$E_{\rm F}$(e)/MeV	$\langle E_n\rangle$/MeV	ζ
SGR 1806-20	24	162.93	78.46	4.104×10^{-3}
SGR 1900+14	7.0	119.73	71.62	2.978×10^{-3}
SGR 0526-66	5.6	113.24	70.54	6.373×10^{-3}
CXOU J0100	3.9	103.45	68.87	1.55×10^{-3}
1E 2259+586	0.59	64.51	61.23	>1
4U 0142+61	1.3	78.60	64.27	>1
1E$^{\rm d}$1048.1-5937	4.2	105.38	69.21	6.313×10^{-4}
1E 1841-045	7.1	120.16	71.69	4.829×10^{-3}
1RXSJ 1708	4.7	108.27	69.72	1.542×10^{-2}
CXO$^{\rm t}$J1647	1.6	82.79	65.09	1.321×10^{-1}

From Table 5, ζ is in the range of 10^{-3}–10^{-2} for most of the magnetars. The exceptions are CXO J1647, 4U 0142+61, and 1E 2259+586. The possible explanations are presented as follows.

(I) For the transient magnetar CXO J1647, its luminosity $L_{\rm X}$ can be associated with bursting activities,[10] so its observed value of $L_{\rm X}$ is much larger than that obtained from the calculation using our model. Its ζ is thus higher than that of most confirmed magnetars.

(II) As for 4U 0142+61, the simplest explanation for its high $L_{\rm X}$ involves a low-mass X-ray binary with a very faint companion as analogous to 4U 1627-67.[51] The observed properties of 1E 2259+586 are consistent with the suggestion that it is an isolated pulsar undergoing a combination of spherical and disk accretions.[52] This magnetar can be powered by the accretion from the remnant of Thorne–Zytow object[20] or by a fall-back disk.[24]

(III) For magnetars 4U 0142+61 and 1E 2259+586 with abnormal values of ζ ($\zeta > 1$), their persistent soft X-ray/γ-ray emissions are related to the accretion, which is beyond the scope of our model. Therefore, these two sources together with CXOJ1647 should not be considered further in the following discussion.

Since the value of ζ is mainly determined by the magnetic field of the magnetar, the average value of ζ for the remaining confirmed magnetars can be approximately calculated as

$$\langle\zeta\rangle = \frac{\sum B_i\zeta_i}{\sum B_i}. \tag{23}$$

Employing Eq. (22) gives the value of $\langle\zeta\rangle$ for the confirmed magnetars, $\langle\zeta\rangle \sim 5.493\times10^{-3}$. If the observed soft X-ray/γ-ray output of a magnetar is dominated by the transport of the magnetic field energy through the core, then the (total) neutrino loss will exceed the surface flux by a factor of ~ 30.[18,21] As we know, a common energy convertor gives an efficiency of $\sim$ (25–55)%. Thus, the value of $\langle\zeta\rangle$ is estimated to be 10^{-4}, if we consider the thermal energy loss caused by the

absorption of heat by the star's inner matter. Thus our calculation result of $\langle\zeta\rangle$ is reasonable and feasible.

4.4. Comparing calculations with observations

Theoretically, $\langle\zeta\rangle$ allows us to calculate the value of $L_{\rm X}$ in any superhigh magnetic field. Inserting the value of $\langle\zeta\rangle$ into Eq. (22) gives the value of $L_{\rm X}$ under certain conditions. The main calculation results can be summarized as follows. When B is assumed to be 1.0 $\times10^{14}$–3.0 $\times10^{15}$ G, $L_{\rm X}$ is 5.232 $\times$ 10^{31}–1.152 $\times10^{37}$ erg·s^{-1} correspondingly. In Table 6, we partly list the ultimately determined values of $L_{\rm X}$ of the magnetars.

Table 6. Theoretical luminosities $L_{\rm X}$ of magnetars.

$B/10^{14}$ G	B^*	$E_{\rm F}$(e)/MeV	$\langle E_\nu\rangle$/MeV	$\langle E_{\rm n}\rangle$/MeV	$L_{\rm X}$/erg·s^{-1}
2.0	4.53	87.54	22.15	66.01	4.273 $\times10^{33}$
4.0	9.06	104.10	35.72	68.99	3.971 $\times10^{34}$
8.0	18.12	123.80	52.12	72.29	3.561 $\times10^{35}$
10	22.66	130.90	58.07	73.44	6.740 $\times10^{35}$
20	45.31	155.67	78.94	77.34	4.241 $\times10^{36}$
25	56.63	164.60	86.60	78.71	7.393 $\times10^{36}$

Furthermore, employing the average value of ζ, we also produce a diagram of $L_{\rm X}$ as a function of B. The numerical results agree well with the observational data for the magnetars, as shown in Fig. 2.

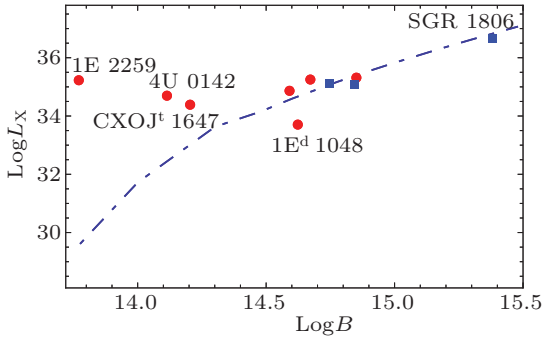


Fig. 2. (colour online) The $L_{\rm X}$ of magnetars as a function of B when $Y_{\rm e} = 0.05$ and $\rho = \rho_0$. Circles and squares are for AXPs and SGRs, respectively. The range of B is assumed to be form 0.6 $\times$ 10^{14} G to 3.0$\times10^{15}$ G.

In Fig. 2, the magnetars listed are distributed around the curve except for 4U 0142+61, 1E 2259+586, CXO J1647, and 1E 1048.1-5937. The luminosity $L_{\rm X}$ obviously increases with the increase of B, and the slope of the curve is larger at weaker fields ($B < 3.0\times10^{14}$ G). This comes out as we have anticipated, because Eq. (1) holds approximately only when $B \gg B_{\rm cr}$. In other words, the stronger the magnetic field, the smaller the calculation error.

As for 1E$^{\rm d}$1048.1-5937 with the lowest value of ζ, this object was detected as a 6.4 s dim isolated pulsar near the Carina Nebula,[53] substantial data were subsequently obtained, showing unambiguous evidence for a large flux increase coupled to a decrease in the pulsed fraction[54] and that its $L_{\rm X}$ decreased from $(1.0 \sim 2.0)\times10^{34}$ erg·s^{-1} to 5.4×10^{33} erg·s^{-1} between September 2004[54] and August 2011. Therefore, the observed value of $L_{\rm X}$ is far less than its theoretically calculated value, and is well below the fitted curve.

For transient magnetars XTE J1810-197, 1E 1547.0-5408, and SGR 1627-41 (not illustrated in Fig. 2), their observed soft X-ray luminosities are much higher than those calculated using our model, the possible explanations may be summarized as follows.

I) XTE J1810-197, discovered in 2003, displayed a persistent flux enhancement by a factor larger than 100.[55] The quiescent level of luminosity $L_{\rm X}$ increased from 7.0×10^{32} erg·s^{-1} to 5.0×10^{34} erg·s^{-1} between June 1992 and September 2004.[56,57] The latest observations, however, showed an obvious decline in $L_{\rm X}$ ($L_{\rm X} \sim 1.9\times10^{32}$ erg·s $^{-1}$ at present).

II) For magnetars SGR 1627-41, CXO J1647, and 1E 1547.0-5408, when they shine, their spectral properties are similar to those of the persistent sources. During their quiescent phases, they universally possess $L_{\rm X} \sim 10^{32}$ erg·s^{-1} and soft thermal spectra, which make them similar to central compact objects.[58] Their long-term variations in $L_{\rm X}$ could be associated with bursts. The source high state coincided with a period of strong bursting activity, while in the following years, its luminosity decreased because no burst is emitted.[10]

III) With respect to SGR 1627-41, more than 100 bursts were observed by various satellites over a period of about 6 weeks in 1998.[16] Its soft X-ray counterpart was identified in 1998, with $L_{\rm X}$ of 10^{35} erg·s^{-1}. How-

ever, no bursts have been reported since then. Observations carried out in the following 13 years demonstrated a monotonic decrease in its $L_{\rm X}$, and its current $L_{\rm X}$ is about 2.5×10^{33} erg·s^{-1} (see in Table 4).

IV) For those four magnetars, their magnetic fields are concentrated in a narrow range of (1.6–2.2)$\times10^{14}$ G, correspondingly, their calculated values of $L_{\rm X}$ are in the range of (10^{30}–10^{33}) erg·s^{-1} according with our model. It is not strange that the observed value of $L_{\rm X}$ of a transient magnetar is far higher than that calculated if we take into account the long-term effects of the bursting activities on its luminosity.

With respect to SGR 1806-20, its observed value of $L_{\rm X}$ may be biased by the intense low-frequency absorption, corresponding to an electron column density of $\sim 6\times10^{22}$ cm^{-2},[59,60] as a result, a significant blackbody component contained in the X-ray bolometric flux is undetected, the luminosity in relativistic particles needed to power the plerion is $\sim 5.0\times10^{36}\times(D/8\ {\rm kpc})^{2.5}$ erg·s^{-1}.[50] In order to reduce the calculation error, we make use of the $L_{\rm X}$ cited from Ref. [50], which agrees well with the curve shown in Fig. 2.

Finally, the timing observations show that the value of $\dot{P}$ of SGR 0418+5729 is less than 6.0×10^{-15} s·s^{-1}, which implies that the surface dipolar magnetic field of SGR 0418+5729 is lower than 7.5×10^{12} G.[49] If the observations are reliable, then the calculated value of $L_{\rm X}$ of SGR 0418+5729 is far less than the observed value of a canonic magnetar ($\sim$ (10^{32}–10^{36}) erg·s^{-1}) according to our model. Therefore, we can state that our model does not contradict the observations (so far, the real value of $L_{\rm X}$ of SGR 0418+5729 is too low to be observed). SGR 0418+5729 may present a new challenge to the magnetar model.

5. Conclusion

In this paper, we provide a mechanism for magnetar soft X-ray/γ-ray emission, compute the luminosity $L_{\rm X}$ on theoretical grounds, generate a diagram of $L_{\rm X}$ versus B, and compare our results with magnetar observations. Our main conclusions are as follows.

(A) Superhigh magnetic fields give rise to an increase in $E_{\rm F}$(e), which will induce EC inside the magnetar. The $^3{\rm P}_2$ neutron Cooper pairs with $\Delta_{\max}(^3{\rm P}_2)\sim0.048$ MeV will be destroyed by the high-energy neutrons produced by the EC through the interaction of nuclear force.

(B) In anisotropic neutron superfluid, the $^3{\rm P}_2$ neutron Cooper pair has magnetic energy $2\mu_{\rm n}B$ due to its magnetic momentum $2\mu_{\rm n}$ in the applied magnetic field. While being destroyed by the outgoing high-energy neutrons, the magnetic moments of the $^3{\rm P}_2$ neutron Cooper pairs are no longer arranged in the paramagnetic direction, then the magnetic energy (the magnetic energy element is $2\mu_nB$) will be released.

(C) The magnetic energy released then will be transformed into the thermal energy. While accumulating to a certain degree, the overwhelming majority of the thermal energy transformed will be absorbed by the inner matter or released in the form of neutrinos.

(D) A small fraction of this heat is transported from the interior to the surface by heat conduction. It then can be radiated in the form of photons from the surface. After a highly efficient modulation within the star's magnetosphere, this surface thermal emission is shaped into a spectrum of soft X-ray/γ-ray with the observed characteristics of the magnetars.

Finally, despite previous research, the existing analysis is approximate, and many assumptions are invoked consequently. Because our computational methods are completely new approaches, they need to be empirically validated. It is earnestly hoped that our calculations can soon be combined with the latest studies and observations of magnetars to present a deeper understanding of the nature of soft X-ray/γ-ray emission of the magnetars.

References

[1] Duncan R C and Thompson C 1992 *Astrophys. J.* **392** 9

[2] Thompson C and Duncan R C 1993 *Astrophys. J.* **543** 340

[3] Thompson C and Duncan R C 1995 *Mon. Not. R. Astron. Soc.* **275** 255

[4] Gao Z F, Wang N, Yuan J P, Jiang L, Song D L and Qiao E L 2011 *Astrophys. Space Sci.* **333** 427

[5] Hurley K, Boggs S E, Smith D M, Duncan R C, Lin R, Zoglauer A, Krucker S, Hurford G, Hudson H, Wigger C, Hajdas W, Thompson C, Mitrofanov I, Sanin A, Boynton W, Fellows C, von Kienlin A, Lichti G, Rau A and Cline T 2005 *Nature* **434** 1098

[6] Peng Q H and Tong H 2007 *Mon. Not. R. Astron. Soc.* **378** 159

[7] Peng Q H and Tong H 2009 *Proceedings of the 10th Symposium on Nuclei in the Cosmos* 27 July 2008 Mackinac Island, USA, p. 189

[8] Mereghetti S, De Luca A, Caraveo P A, Becker W, Mignani R and Bignami G F 2002 *Astrophys. J.* **581** 1280

[9] Halpern J P, Gotthelf E V, Beckek R H, Helfand D J and White R L 2005 *Astrophys. J. Lett.* **632** 29

[10] Mereghetti S 2008 *arXiv*: 0804.0250v1 [astro-ph]

[11] Mereghetti S, Tiengo A, Esposito P, Götz D, Stella L, Israel G L, Rea N, Feroci M, Turolla R and Zane S 2005 *Astrophys. J.* **628** 938

[12] Tong H, Xu R X, Peng Q H and Song L M 2010 *Research Astron. Astrophys.* **10** 553

[13] Thompson C, Lyutikov M and Kulkarni S R 2002 *Astrophys. J.* **574** 332

[14] Heyl J S and Hernquist L 1997 *Astrophys. J.* **489** 67

[15] Rheinhardt M and Geppert U 2003 *Phys. Rev. Lett.* **88** 10

[16] Woods P M and Thompson C 2004 *arXiv*: astro-ph/0406133

[17] Pons J A, Link B, Miralles J A and Geppert U 2007 *Phys. Rev. Lett.* **98** 1101

[18] Lyutikov M and Gavriil F P 2006 *Mon. Not. R. Astron. Soc.* **368** 690

[19] Nobili L, Turolla R and Zane S 2008 *Mon. Not. R. Astron. Soc.* **386** 1527

[20] van Paradijs J, Taam R E and van den Heuvel E P J 1995 *Astron. Astrophys.* **299** 41

[21] Ghosh P, Angelini L and White N E 1997 *Astrophys. J.* **478** 713

[22] Alpar M A 2001 *Astrophys. J.* **554** 1245

[23] Tong H, Song L M and Xu R X 2010 *Astrophys. J. Lett.* **725** 196

[24] Ertan Ü and Erkut M H 2008 *Astrophys. J.* **673** 1062

[25] Ertan Ü, Göğüş E and Alpar M A 2006 *Astrophys. J.* **640** 345

[26] Thompson C and Beloborodov A M 2005 *Astrophys. J.* **634** 565

[27] Beloborodov A M and Thompson C 2007 *Astrophys. J.* **657** 967

[28] Lamb D Q and Pethick C J 1976 *Astrophys. J. Lett.* **209** 77

[29] Mazurek T J 1976 *Astrophys. J. Lett.* **207** 87

[30] Langanke K and Martinez-Pindo G 2000 *Nucl. Phys.* A **673** 481

[31] Peng Q H 2001 *Progress in Physics* **21** 225 (in Chinese)

[32] Luo Z Q, Liu M Q, Peng Q H and Xie Z H 2006 *Chin. J. Astron. Astrophys.* **6** 455

[33] Gao Z F, Peng Q H, Wang N and Chou C K 2011 *A Dispute on the Electron Fermi Energy in Intense Magnetic Fields*

[34] Gao Z F, Wang N, Yuan J P, Jiang L and Song D L 2011 *Astrophys. Space Sci.* **332** 129

[35] Shapiro S L and Teukolsky S A 1983 *Black Holes, White Drarfs, and Neutron Stars* (New York: John Wiley & Sons)

[36] Bardeen J, Cooper L N and Schrieffer J R 1957 *Phys. Rev.* **108** 1175

[37] Amundsen L and Østgard E 1985 *Nucl. Phys.* A **437** 487

[38] Schaab C, Weber F, Weigel M K and Glendenning N K 1996 *Nucl. Phys.* A **605** 531

[39] Elgarøy Ø, Engvik L, Hjorth-Jensen M and Osnes E 1996 *Nucl. Phys.* A **607** 425

[40] Elgarøy Ø, Engvik L, Hjorth-Jensen M and Osnes E 1996 *Phys. Rev. Lett.* **77** 1428

[41] Horvath J E and Allen M P 2011 *arXiv*: 1104.2875v1

[42] Hou Q W, Cao B Y and Guo Z Y 2009 *Acta Phys. Sin.* **58** 7809 (in Chinese)

[43] Wang J, Li J Y and Zhang Z G 2010 *Acta Phys. Sin.* **59** 476 (in Chinese)

[44] Wu Z C 2010 *Acta Phys. Sin.* **59** 6326 (in Chinese)

[45] Jiang T, Ouyang J, Liu X J, Zhang L and Ren J L 2011 *Acta Phys. Sin.* **60** 090206 (in Chinese)

[46] Gao X Y and Zhang Z G 2011 *Acta Phys. Sin.* **60** 044401 (in Chinese)

[47] Pang W Z, Yang X J and Xie Z K 2011 *Chin. Phys.* B **20** 049701

[48] Zhang S L, Liu F S, Peng X J, Zhang M J, Li Y H, Ma X J and Xue X D 2011 *Acta Phys. Sin.* **60** 014401 (in Chinese)

[49] Rea N, Esposito P, Turolla R, Tiengo A, Götz D, Göğüş E and Kouveliotou C 2010 *Science* **330** 944

[50] Thompson C and Duncan R C 1996 *Astrophys. J.* **473** 322

[51] Israel G L, Mereghetti S and Stella L 1994 *Astrophys. J.* **433** 25

[52] White N E and Marshall F E 1984 *Astrophys. J.* **281** 354

[53] Steward F, Charles P A and Smale A P 1986 *Astrophys. J.* **305** 814

[54] Mereghetti S, Tiengo A, Stella L, Israel G L, Rea N, Zane S and Oosterbroek T 2004 *Astrophys J.* **608** 427

[55] Ibrahim A I, Markwardt C B, Swank1 J H, Ransom S, Roberts M, Kaspi V, Woods P M, Safi-Harb S, Balman S, Parke W C, Kouveliotou C, Hurley K and Cline T 2004 *Astrophys. J. Lett.* **609** 21

[56] Bernardini F, Israel G L and Dall'Osso S 2009 *Astron. Astrophys.* **498** 195

[57] Gotthelf E V, Halpern J P, Buxton M and Bailyn C 2004 *Astrophys. J.* **605** 368

[58] Mereghetti S 2010 *arXiv*: 1008.2891v1[astro-ph.HE]

[59] Murakami T, Tanaka Y, Kulkarni S R, Ogasaka Y, Sonobe T, Ogawara Y, Aoki T and Yoshida A 1994 *Nature* **368** 127

[60] Sonobe T, Murakami T, Kulkarni S R, Aoki T and Yoshida A 1994 *Astrophys. J.* **436** 23